The EMBO Journal vol.11 no.3 pp.863-874, 1992

Endocytosis of glycophospholipid-anchored and transmembrane forms of CD4 by different endocytic pathways

Gilbert-André Keller[1], Mark W.Siegel[1] and Ingrid W.Caras[2,3]

Departments of [1]Pharmaceutical Sciences and [2]Immunobiology, Genentech, Inc., 460 Point San Bruno Boulevard, South San Francisco, CA 94080, USA

[3]Author to whom correspondence should be addressed

Communicated by D.Louvard

A glycophosphatidylinositol (GPI)-anchored form of the CD4 receptor was constructed by fusing the extracellular domain of CD4 to the COOH-terminus of decay accelerating factor (DAF), containing a signal for GPI-anchor attachment. The internalization of GPI-linked CD4 (CD4DAF) was compared to that of transmembrane CD4 using both [^{125}I]gp120 and anti-CD4 antibodies. We show that transmembrane CD4 is rapidly endocytosed in transfected CHO cells, while CD4DAF is internalized at a rate ~3-fold slower. Immunoelectron microscopy suggests that whereas transmembrane CD4 is endocytosed via clathrin-coated vesicles, CD4DAF enters cells by an alternative pathway involving non-coated microinvaginations of the plasma membrane. Following internalization CD4DAF recycles through a primaquine-insensitive compartment, whereas the recycling of transmembrane CD4 is inhibited by primaquine, suggesting that the two receptors may recycle from distinct populations of early endosomes. Co-localization of both CD4DAF and CD4 with an antibody against a lysosomal membrane protein suggests that the two endocytic pathways may converge.

Key words: endocytosis/glycophosphatidylinositol membrane anchor

Introduction

A small subset of integral membrane proteins is anchored to the plasma membrane not by a transmembrane domain, but by a glycophosphatidylinositol (GPI) structure covalently attached to the COOH-terminus of the protein [for reviews see Ferguson and Williams (1988); Low (1989) and Cross (1990)]. GPI-anchor attachment is thought to occur in the endoplasmic reticulum (Bangs *et al.*, 1985, 1986; Ferguson *et al.*, 1986) and is directed by a signal at the COOH-terminus of the protein (Caras *et al.*, 1987). The GPI-anchored protein is then transported to the cell surface via the Golgi apparatus.

Only a few studies have focused on the fate of GPI-anchored proteins following their arrival at the cell surface. The GPI-linked folate receptor in MAI04 cells was recently found to cluster and recycle at the cell surface in non-coated invaginations resembling caveolae, but without entering endosomes or lysosomes (Rothberg *et al.*, 1990). 5'-Nucleotidase, on the other hand, appears to recycle between the cell surface and an endosomal compartment in rat hepatoma cells (van den Bosch *et al.*, 1988). A study of decay accelerating factor (DAF) on human polymorphonuclear cells suggested that DAF is partially internalized and partially shed from the plasma membrane into the fluid phase (Tausk *et al.*, 1989), while Thy-1 appears to be very stable on the surface of murine lymphoma cells, possibly undergoing slow, limited endocytosis (Lemansky *et al.*, 1990). These studies provide a confusing picture and suggest that the extracellular domain and/or the cell type may play a role in determining the fate of GPI-linked proteins at the cell surface.

The mechanism whereby GPI-anchored proteins might be internalized is unknown. Clustering and endocytosis in clathrin-coated pits is thought to require signals in the cytoplasmic domains of integral membrane proteins (Davis *et al.*, 1987; Iacopetta *et al.*, 1988; Lazarovits and Roth, 1988), which are lacking in GPI-linked proteins. Consistent with this, the GPI-anchored protein, Thy-1 (Low and Kincade, 1985), has been found to be excluded from clathrin-coated pits (Bretscher *et al.*, 1980).

The CD4 receptor is an ~55 kDa transmembrane glycoprotein found on the surface of a subset of T-lymphocytes (Maddon *et al.*, 1985). The CD4 molecule binds to class II major histocompatibility complex (MHC) molecules and acts as the cellular receptor for the human immunodeficiency virus (HIV-1) by binding with high affinity to gp120, the major envelope glycoprotein of HIV-1 (Klatzman *et al.*, 1984; McDougal *et al.*, 1986). In this report, we examine the consequences on endocytosis of substitution of the transmembrane-cytoplasmic domains of CD4 with a GPI membrane anchor. This was achieved by fusing the last 37 amino acids of DAF, containing a signal for GPI-anchor attachment (Caras *et al.*, 1987, 1989), to the extracellular domain of CD4. This system offers the advantage of being able to compare directly the fate of the same extracellular domain anchored to the plasma membrane by a GPI membrane anchor versus a transmembrane-cytoplasmic domain. We show that transmembrane CD4 expressed in Chinese hamster ovary (CHO) cells is endocytosed via clathrin-coated pits, whereas GPI-linked CD4 enters cells by a slower, clathrin-independent pathway.

Results

Replacement of the transmembrane-cytoplasmic domains of CD4 with a GPI membrane anchor

Using gene manipulation, we constructed a CD4DAF fusion protein in which the last 65 amino acids of CD4 [encoding the transmembrane and cytoplasmic domains (Maddon *et al.*, 1985)] were replaced with the last 37 amino acids of DAF, containing the signal for GPI-anchor attachment (Caras *et al.*, 1987, 1989) (Figure 1A). A cDNA encoding this protein was transiently expressed in 293 cells together with full-length native CD4 and CD4T, a truncated form of CD4

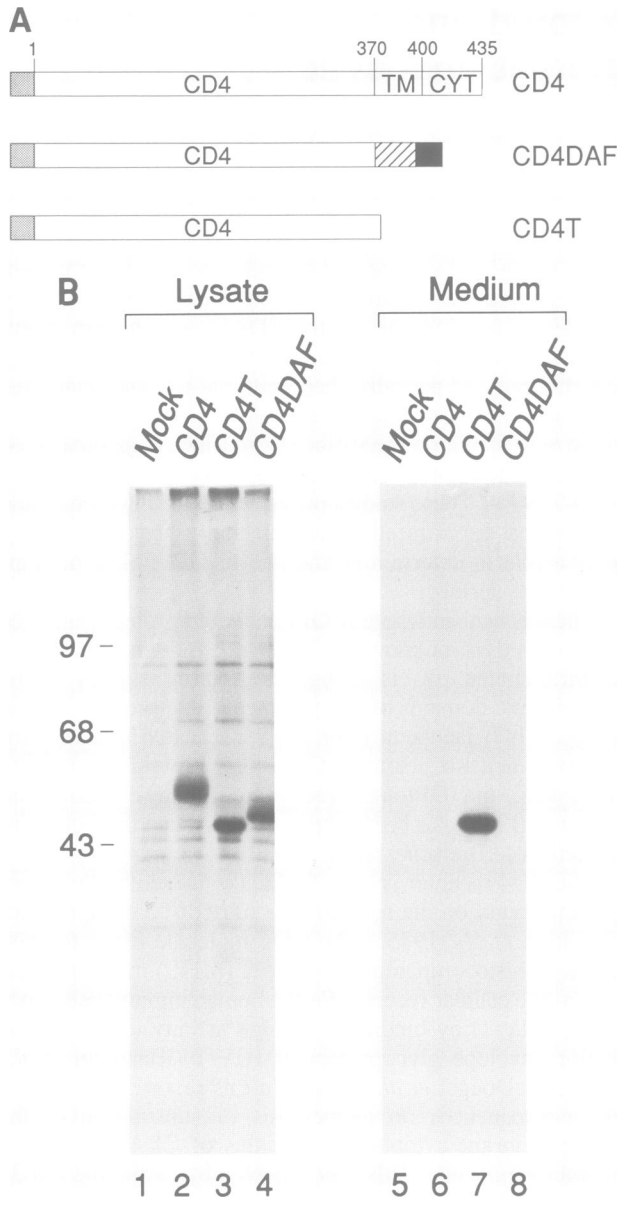

Fig. 1. (**A**) Schematic diagram showing transmembrane CD4, the CD4DAF fusion protein and truncated CD4, designated CD4T. The unshaded box represents the extracellular domain of CD4 (residues 1–370). TM is the transmembrane domain and CYT is the cytoplasmic domain. Shaded areas are as follows: (▨) CD4 signal peptide; (■) COOH-terminal hydrophobic domain of DAF (residues 331–347) (Caras *et al.*, 1989); (▨) additional DAF sequence required for GPI attachment (residues 321–330) (Caras *et al.*, 1989). (**B**) Immunoprecipitation of CD4 proteins from [^{35}S]methionine-labeled transfected 293 cells. Cells were labeled with [^{35}S]methionine 24 h after transfection with DNAs encoding CD4 proteins as indicated. CD4 was immunoprecipitated from cell lysates (lanes 1–4) and culture media (lanes 5–8) using an anti-CD4 monoclonal antibody. DNA was omitted from the mock-transfected control culture.

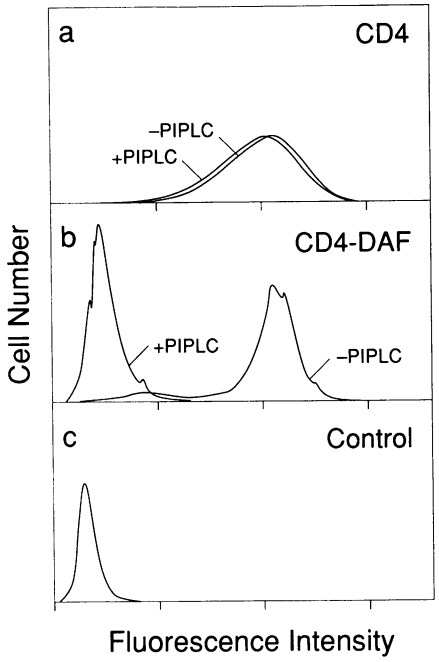

Fig. 2. Release of cell-surface CD4DAF by PIPLC. Stably transfected CHO cells expressing either native CD4 (**panel a**) or CD4DAF (**panel b**) were incubated for 60 min at 37°C in the presence or absence of purified PIPLC from *B.thuringiensis* as indicated, and then analyzed by indirect immunofluorescence and flow cytometry. **Panel c** shows the fluorescence intensity of non-transfected control cells.

lacking the transmembrane and cytoplasmic domains (Smith *et al.*, 1987). Transfected cells were labeled with [^{35}S]methionine 24 h after transfection, and CD4 was immunoprecipitated from the cell extracts and culture media using a monoclonal antibody against CD4 (Figure 1B). As expected, the 55 kDa native CD4 was localized exclusively in the cell lysate while the truncated form (CD4T) which lacks a transmembrane domain, was secreted into the culture medium as has been described previously (Smith *et al.*, 1987). The CD4DAF fusion protein, containing the extracellular domain of CD4 fused to a GPI-anchor attachment signal, was cell associated.

To show that the cell-associated CD4DAF is targeted to the plasma membrane and is anchored by a GPI-anchor, CHO cells stably transfected with either CD4 or CD4DAF were analyzed by fluorescence flow cytometry (FACS) before and after treatment with purified phosphatidylinositol-specific phospholipase C (PIPLC) from *Bacillus thuringiensis*. The marked shift in the fluorescence intensity of transfected cells relative to non-transfected control cells indicated that the CD4DAF fusion protein is on the cell surface, as is native CD4 (Figure 2). Treatment with PIPLC dramatically reduced the amount of cell-surface CD4DAF, as indicated by the large decrease in relative cell fluorescence (Figure 2, panel b). In contrast, the levels of native CD4 were unaffected by PIPLC. These data indicate that fusion of the extracellular domain of CD4 to the GPI-anchor attachment signal of DAF produces a GPI-anchored form of CD4 on the cell surface.

Binding of [^{125}I]gp120

To determine whether substitution of a GPI-anchor affects the ligand-binding properties of CD4, cells expressing either native CD4 or CD4DAF were incubated with [^{125}I]gp120 (130 000 c.p.m.; 11 000 c.p.m./ng) in the presence of increasing concentrations of rgp120, and a standard Scatchard analysis was performed (Figure 3A). Non-specific binding to non-transfected CHO cells was negligible. There was no significant difference in the affinity of gp120 for CD4 ($K_d = 3 \times 10^{-8}$ M) versus CD4DAF ($K_d = 4 \times 10^{-8}$ M), indicating that the ligand-binding properties of the receptor are unaffected by the mode of attachment to the membrane.

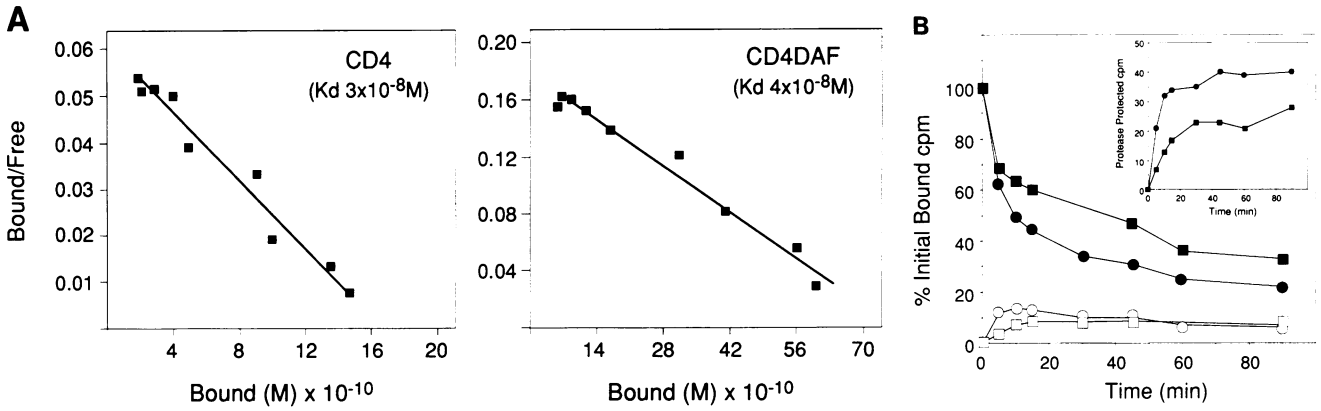

Fig. 3. (**A**) Scatchard plot of the binding of [^{125}I]gp120 to cells expressing CD4 or CD4DAF. The Scatchard plot was constructed using a modification of the program system 'Ligand' (Munson and Rodbard, 1980). (**B**) Internalization of [^{125}I]gp120 at 37°C. Stably transfected CHO lines expressing CD4 or CD4DAF were incubated with [^{125}I]gp120 for 2 h at 4°C, washed with cold medium and then rapidly warmed to 37°C. At various times samples were chilled, the cells and media were separated, and the cells were treated with subtilisin to remove surface label. Closed symbols, total cell-associated radioactivity as a percentage of the amount initially bound at 4°C; ●, CD4; ■. CD4DAF; open symbols, intracellular (subtilisin-resistant) radiolabel as a percentage of the amount initially bound at 4°C; ○, CD4; □, CD4DAF. Insert, intracellular (subtilisin-resistant) radioactivity expressed as a percentage of the total amount of cell-associated at each time point; ●, CD4; ■, CD4DAF. Shown is a representative of four experiments.

Kinetics of internalization of [^{125}I]gp120

To determine the effect on endocytosis of replacement of the transmembrane-cytoplasmic domains of CD4 with a GPI-anchor, we compared the ability of both CD4DAF and CD4 to internalize the ligand, [^{125}I]gp120. Stably transfected CHO cells expressing either CD4 or CD4DAF were saturated with [^{125}I]gp120 by incubation with radioiodinated rgp120 (2 μg/ml, 33 nM, ~8700 c.p.m./ng) for 2 h at 4°C. Specifically bound [^{125}I]gp120 was determined by subtracting the amount of [^{125}I]gp120 bound in the presence of 600 μg/ml of unlabeled rgp120 (a 300-fold excess) from the total radiolabel bound in the absence of added rgp120. Typically, specific binding of [^{125}I]gp120 was 98.2–98.4% of the total binding. For these experiments we selected CHO clones (expressing CD4 or CD4DAF) that bound similar levels of [^{125}I]gp120 (~120 000 molecules/cell).

Upon warming of the cells to 37°C, the total amount of cell-associated [^{125}I]gp120 decreased rapidly, as has been observed for other receptor–ligand interactions (Anderson *et al.*, 1981; Mellman and Plutner, 1984) (Figure 3B). Approximately 30–40% of the initially surface-bound [^{125}I]gp120 appeared in the medium, largely in a trichloroacetic acid (TCA)-precipitable form (not shown). A fraction of the bound [^{125}I]gp120 was rapidly internalized, as estimated by resistance of the radiolabel to removal by subtilisin (Figure 3B). (Subtilisin removed 96–97% of the [^{125}I]gp120 from cells held at 4°C where all of the bound radiolabel is presumably on the cell surface.) The difference in the kinetics and degree of internalization of [^{125}I]gp120 bound to CD4DAF versus CD4 was most apparent during the first 15 min after warming. The initial rate of internalization of bound [^{125}I]gp120 was ~2.2%/min for CD4 and ~0.7%/min for CD4DAF. After 10 min at 37°C, ~14% (after background subtraction) of the [^{125}I]gp120 bound to native CD4 was subtilisin resistant versus 7% for radiolabel bound to CD4DAF, and after 30 min a plateau was reached in which ~9% of the [^{125}I]gp120 initially bound either to CD4 or CD4DAF was subtilisin resistant. Figure 3B (inset) shows the proportion of [^{125}I]gp120 inside the cells at various times (subtilisin-resistant radioactivity as a percentage of the total cell-associated, rather than initial bound [^{125}I]gp120), indicating that internalization of gp120 bound to CD4 is faster and more efficient, leveling off after 10–15 min with ~40% of the cell-associated [^{125}I]gp120 resistant to removal by protease.

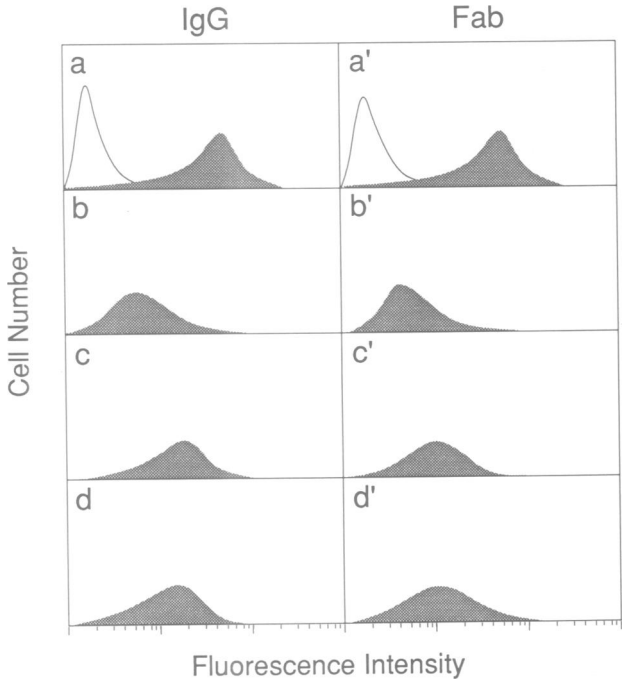

Fig. 4. Recycling of anti-CD4 IgG or Fab fragments bound to CD4DAF. CHO cells expressing CD4DAF were incubated with anti-CD4 IgG or Fab fragments as indicated at 4°C for 60 min. The cells were then warmed to 37°C for 20 min to allow internalization, chilled and incubated with PIPLC for 90 min at 4°C to remove cell-surface CD4DAF. The cells were then returned to 37°C for 0 min (**b,b'**), 10 min (**c,c'**) or 20 min (**d,d'**) to allow recycling. The cells were then incubated with PE-conjugated anti-mouse IgG at 4°C and analyzed by flow cytometry. (**a,a'**) Shaded curve, labeled control cells held on ice for the duration of the experiment and not exposed to PIPLC, indicating the level of anti-CD4 IgG initially bound; unshaded curve, fluorescence intensity of non-transfected CHO cells.

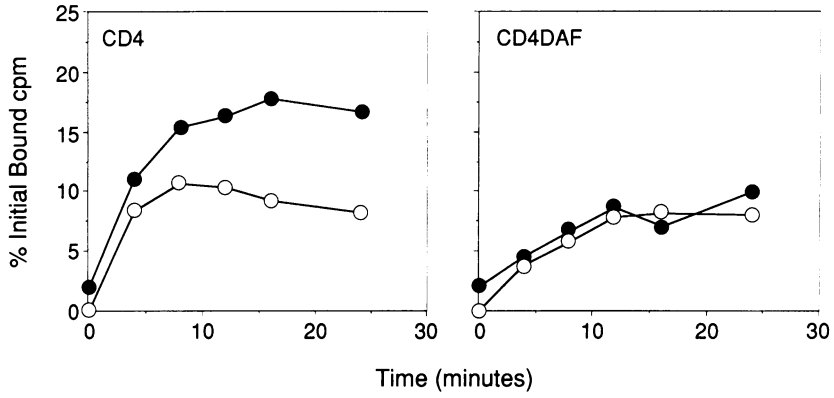

Fig. 5. Effect of primaquine on the endocytosis of [^{125}I]gp120 at 37°C. Cells expressing either CD4 or CD4DAF were incubated with [^{125}I]gp120 for 2 h at 4°C and then washed. Aliquots were subsequently warmed to 37°C in the presence (closed symbols) or absence (open symbols) of 0.6 mM primaquine. At various times, samples were chilled and the cells were treated with subtilisin to remove surface label. Shown is a representative of four experiments.

In contrast, internalization of the gp120–CD4DAF complex reaches a plateau between 30 and 40 min with ~25% of the cell-associated radioactivity protected in an internal compartment. The appearance of a plateau suggests recycling of internalized ligand back to the cell surface.

Recycling of CD4DAF

The above results suggest that both CD4DAF and CD4 may recycle following internalization. Recycling of CD4 has been demonstrated in HeLa and NIH3T3 cells (Pelchen-Matthews *et al.*, 1989). To determine whether CD4DAF recycles, transfected CHO cells were incubated at 4°C with an anti-CD4 monoclonal antibody, or with the corresponding Fab fragment, and then warmed to 37°C for 20 min to allow internalization. CD4DAF–antibody complexes remaining on the cell surface were then removed by incubation with PIPLC at 4°C for 90 min and the cells were again warmed to 37°C for 10 or 20 min to permit recycling. The amount of CD4DAF–IgG complex on the cell surface was then assessed by FACS analysis following incubation with phycoerythrin (PE)-conjugated anti-mouse IgG at 4°C (Figure 4). Control cells were labeled with anti-CD4 IgG and then held on ice for the duration of the experiment. The mean fluorescence of these control cells was measured and designated as 100%. After exposure to PIPLC, the mean fluorescence decreased to ~30%, indicating removal of bound antibody from the cell surface. Similarly, labeled cells that were warmed and then treated with PIPLC had a mean fluorescence of ~30%. Upon rewarming to 37°C, the mean fluorescence of these PIPLC-treated cells increased back to 65 or 52% of control levels for IgG- or Fab-labeled cells, respectively. These data indicate that internalized (PIPLC-resistant) CD4DAF–antibody complexes reappeared on the cell surface during the second warming period, suggesting that CD4DAF is recycled. There was no significant difference in the extent of recycling of Fab fragments versus IgG molecules bound to CD4DAF.

Differential effects of primaquine on the recycling of CD4 and CD4DAF

The weak base primaquine inhibits the recycling of endocytosed transferrin, asialoglycoprotein and MHC glycoproteins, thereby increasing the size of the intracellular pool (Schwartz *et al.*, 1984; Stoorvogel *et al.*, 1987; Reid and Watts, 1990). To determine whether the recycling of CD4 and CD4DAF is similarly affected, we tested the effect of primaquine on the internalization of prebound [^{125}I]gp120. In the presence of primaquine (0.3 or 0.6 mM), the pool of internalized [^{125}I]gp120 bound to CD4 was approximately doubled (Figure 5), increasing from 10 to 18% of the initial bound c.p.m. In contrast, primaquine did not significantly alter the pool of [^{125}I]gp120 internalized via CD4DAF. These data suggest that the intracellular compartments from which CD4 and CD4DAF recycle are distinct, one being primaquine-sensitive while the other is not.

Internalization visualized by immunofluorescence microscopy

To directly visualize the internalization of CD4DAF and CD4 expressed on the surface of CHO cells, we examined the cells by indirect immunofluorescence following a temperature shift from 4 to 37°C. Stably transfected cells were incubated with monoclonal antibodies against CD4 for 1–2 h at 4°C and then warmed to 37°C for 0–60 min to allow internalization. CD4–antibody complexes were localized by indirect immunofluorescence microscopy following fixation, permeabilization and incubation with rhodamine-conjugated anti-mouse IgG. Both CD4 and CD4DAF showed a similar punctate staining pattern on the surface of cells held on ice (Figure 6a). After 5–15 min at 37°C, cells expressing CD4 were uniformly filled with brightly stained endocytic vesicles. By 60 min, the distribution of vesicles was largely perinuclear. In contrast, the endocytosis of CD4DAF complexes was delayed. Fewer endocytic vesicles were visible after 5–15 min of warming and there was significant residual surface staining which obscured events occurring inside the cells. Initially, these vesicles appeared to be localized at the periphery of the cell, in contrast to the uniform distribution seen with CD4-expressing cells. By 30–60 min, the vesicles appeared larger and the distribution was distinctly perinuclear. Staining of non-permeabilized cells indicated that the internalization of anti-CD4 IgG bound to either CD4 or CD4DAF was incomplete, with residual surface label remaining even after 60 min of warming (Figure 6B). This observation is consistent with the conclusion that the receptors recycle. Non-permeabilized cells showed a more diffuse staining

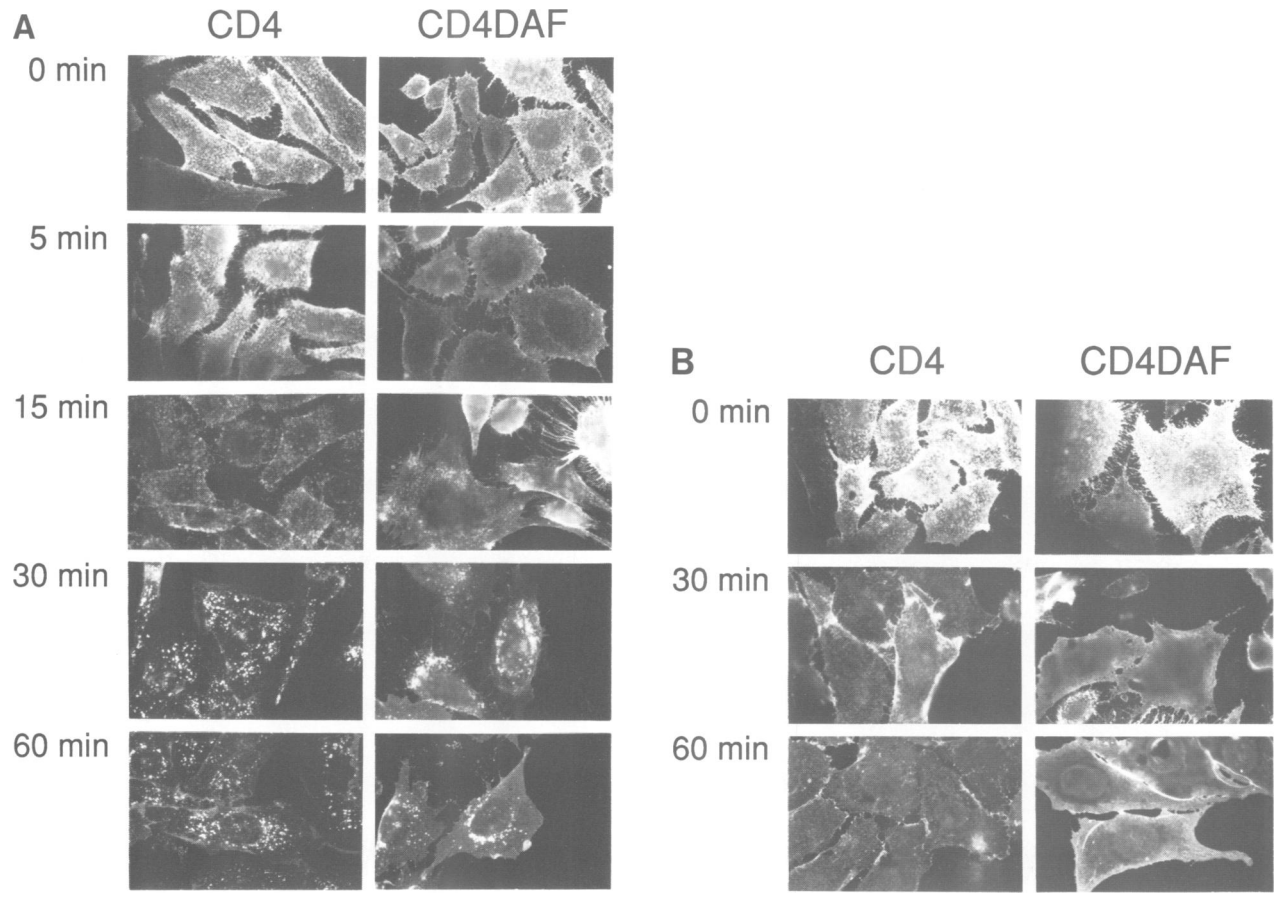

Fig. 6. Internalization of bound anti-CD4 IgG at 37°C, visualized by indirect immunofluorescence. Stably transfected CHO cells, expressing either CD4 or CD4DAF as indicated, were incubated with anti-CD4 monoclonal IgG for 90 min on ice. The cells were then warmed to 37°C for 0–60 min prior to fixation and staining with rhodamine-conjugated anti-mouse IgG. (**A**) Cells were permeabilized prior to staining; (**B**) cells were stained without prior permeabilization. Incubation times at 37°C are as indicated.

pattern after prolonged warming with an absence of punctate or vesicular structures.

The pattern and extent of internalization of CD4DAF during the initial 15 min was difficult to assess in the above experiments because of the high degree of residual surface immunofluorescence. To overcome this difficulty, we again exploited the ability of PIPLC to remove GPI-linked proteins from the cell surface. Cells expressing CD4DAF were incubated with anti-CD4 IgG at 4°C, warmed to 37°C for 0–60 min to allow endocytosis and then incubated with PIPLC for 2 h at 4°C to remove surface complexes. The cells were then fixed and analyzed by indirect immunofluorescence microscopy. Treatment with PIPLC removed most of the surface-bound anti-CD4 IgG from CD4DAF-transfected cells held on ice, while the surface staining of cells expressing CD4 was unaffected by PIPLC (Figure 7). After 7 min of warming, bright clusters of PIPLC-resistant endocytic vesicles were visible at the cell periphery, close to the plasma membrane. With prolonged warming, these vesicles appeared to migrate to the center of the cell, eventually becoming perinuclear. These results indicate that CD4DAF is internalized into an endocytic compartment that is protected from exogenous PIPLC. This process is relatively rapid, internalized vesicles being visible ~7 min after transfer of the cells from 0 to 37°C, and results in an apparent inward migration of endocytic vesicles from the cell surface.

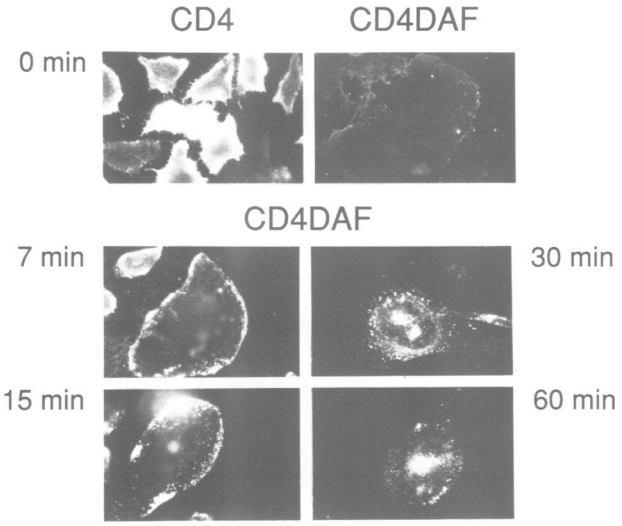

Fig. 7. Internalized anti-CD4 IgG bound to CD4DAF visualized by indirect immunofluorescence after removal of cell-surface complexes by PIPLC. CHO cells expressing CD4DAF or CD4, as indicated, were incubated with anti-CD4 monoclonal IgG for 90 min on ice. The cells were then warmed to 37°C for 0–60 min, chilled and treated with PIPLC for 2 h at 4°C prior to fixation, permeabilization and staining with rhodamine-conjugated anti-mouse IgG. Incubation times at 37°C are as indicated.

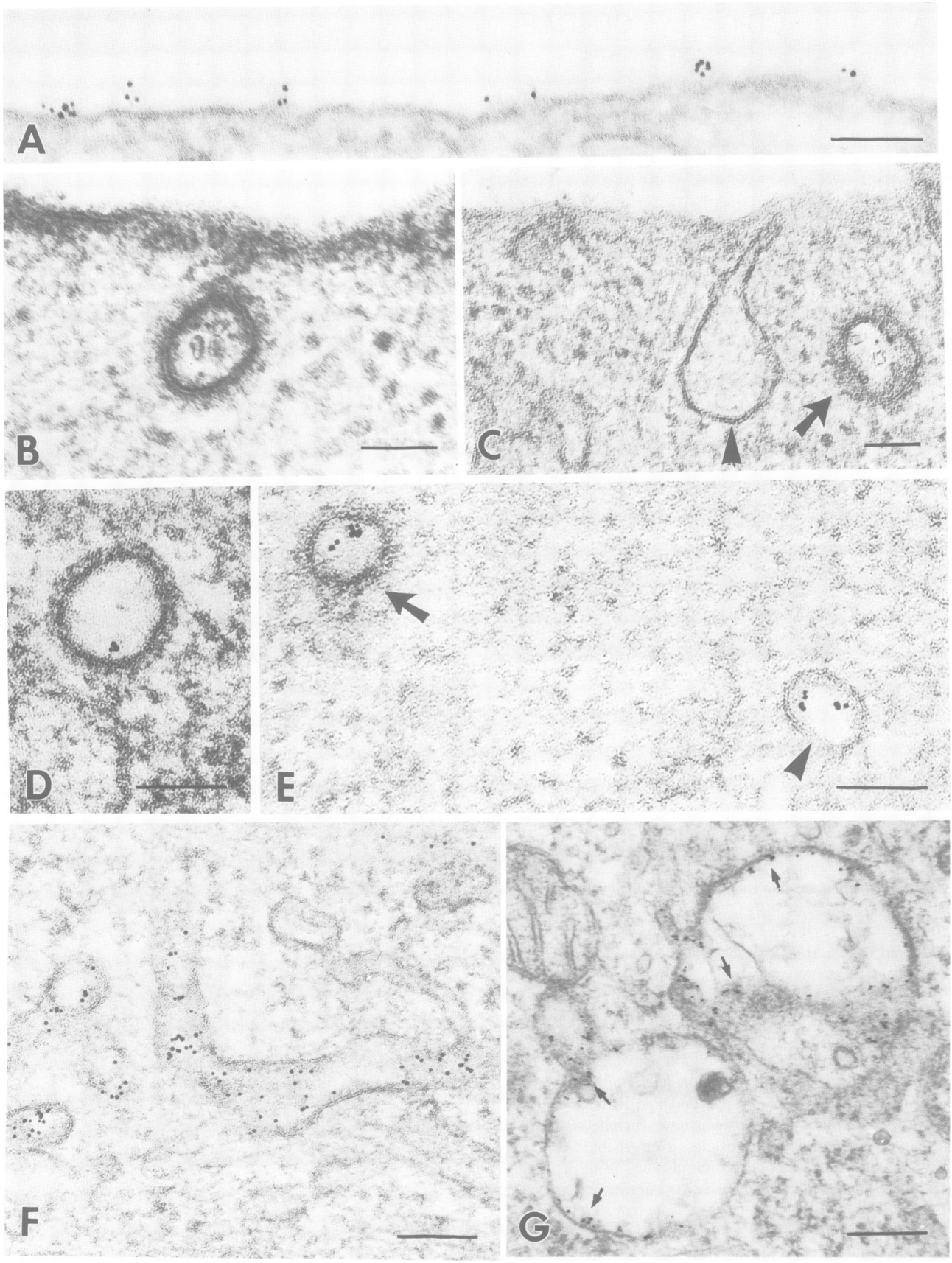

Fig. 8. Localization of CD4 by immunoelectron microscopy. CHO cells expressing CD4 were incubated with anti-CD4 monoclonal IgG followed by 5 nm gold-conjugated anti-mouse IgG at 4°C for 2 h. The cells were then warmed to 37°C for 0–35 min prior to fixation and processing for electron microscopy. Electron micrographs are selected to show the distribution of gold particles on the cell surface at 4°C (**A**), after 5 min at 37°C (**B, C** and **D**), 15 min (**E** and **F**), or 35 min (**G**). (C) A coated vesicle containing gold particles (arrow) is seen next to an empty non-coated pit (arrowhead); (E) CD4 is seen in both coated (arrow) and non-coated (arrowhead) vesicles; intense labeling is seen in tubulo-vesicular structures (F) and in multivesicular bodies (G). Data shown are representative of three experiments. Scale bars = 0.1 μm.

CD4DAF and CD4 enter CHO cells by different endocytic pathways

The apparent difference in the kinetics of internalization and in the immunofluorescence staining patterns, as well as the differential response to primaquine, suggested that CD4DAF and CD4 might be entering the cell by different endocytic pathways. To investigate this, we analyzed the uptake of anti-CD4 IgG by transmission electron microscopy. Cells expressing either CD4DAF or CD4 were incubated with monoclonal anti-CD4 IgG followed by colloidal gold-labeled anti-mouse IgG at 4°C, and then warmed to 37°C for 0–35 min prior to fixation and processing for electron microscopy. Cells expressing either CD4DAF or CD4 showed a generally uniform rather than patched distribution on the plasma membrane and microvilli at 4°C, and the average density of labeling was similar for both cell lines (8.08 gold particles/μm of plasma membrane for CD4 and 8.75 gold particles/μm for CD4DAF) (Figures 8A and 9A). Coated pits and vesicles were seen in the apical cytoplasm, but were unlabeled at 4°C (Table I). Upon warming, CD4

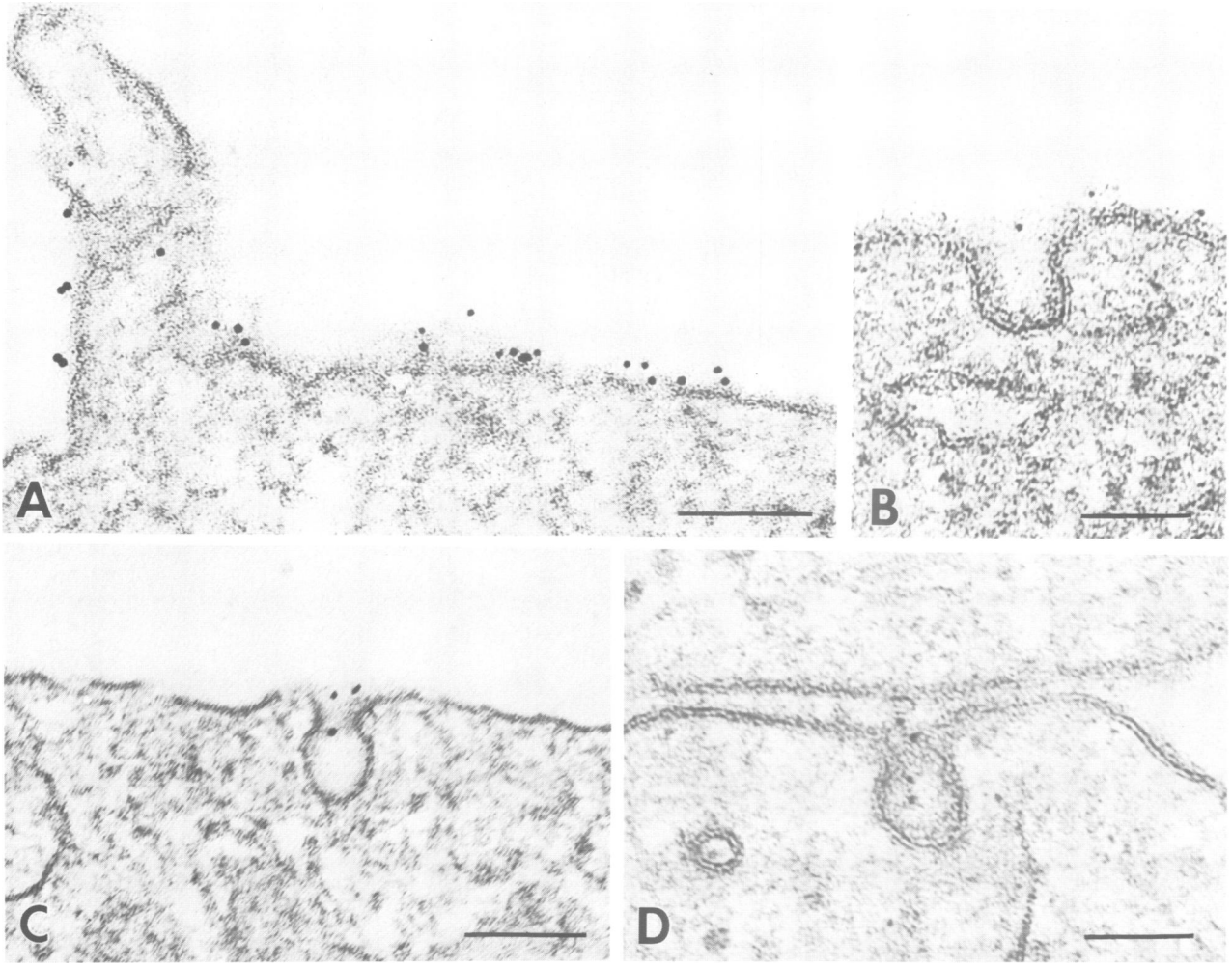

Fig. 9. Localization of CD4DAF by immunoelectron microscopy. CHO cells expressing CD4DAF were treated as described in the legend to Figure 8. Selected electron micrographs show gold particles on the cell surface at 4°C (**A**) and after 10 min at 37°C (**B, C** and **D**). CD4DAF is seen in non-coated pinocytotic invaginations of the plasma membrane (scale bars = 0.1 μm).

Table I. Distribution of gold-labeled CD4 and CD4DAF following endocytosis in CHO cells

	Time at 37°C (min)	Number of vesicles examined		Number of vesicles containing gold particles	
		Coated	Non-coated	Coated	Non-coated
CD4	0	72	57	0	0
	5	97	69	94 (96.9%)[a]	3 (3.1%)
	15	82	87	48 (55.2%)	39 (44.8%)
	35	77	81	5 (6.1%)	76 (93.8%)
CD4DAF	0	47	51	0	0
	5	161	191	0	1
	15	118	97	3 (3.1%)	94 (96.9%)
	35	128	108	4 (3.7%)	104 (96.3%)

[a]Numbers in parentheses show the proportional distribution of label in coated versus non-coated vesicles.

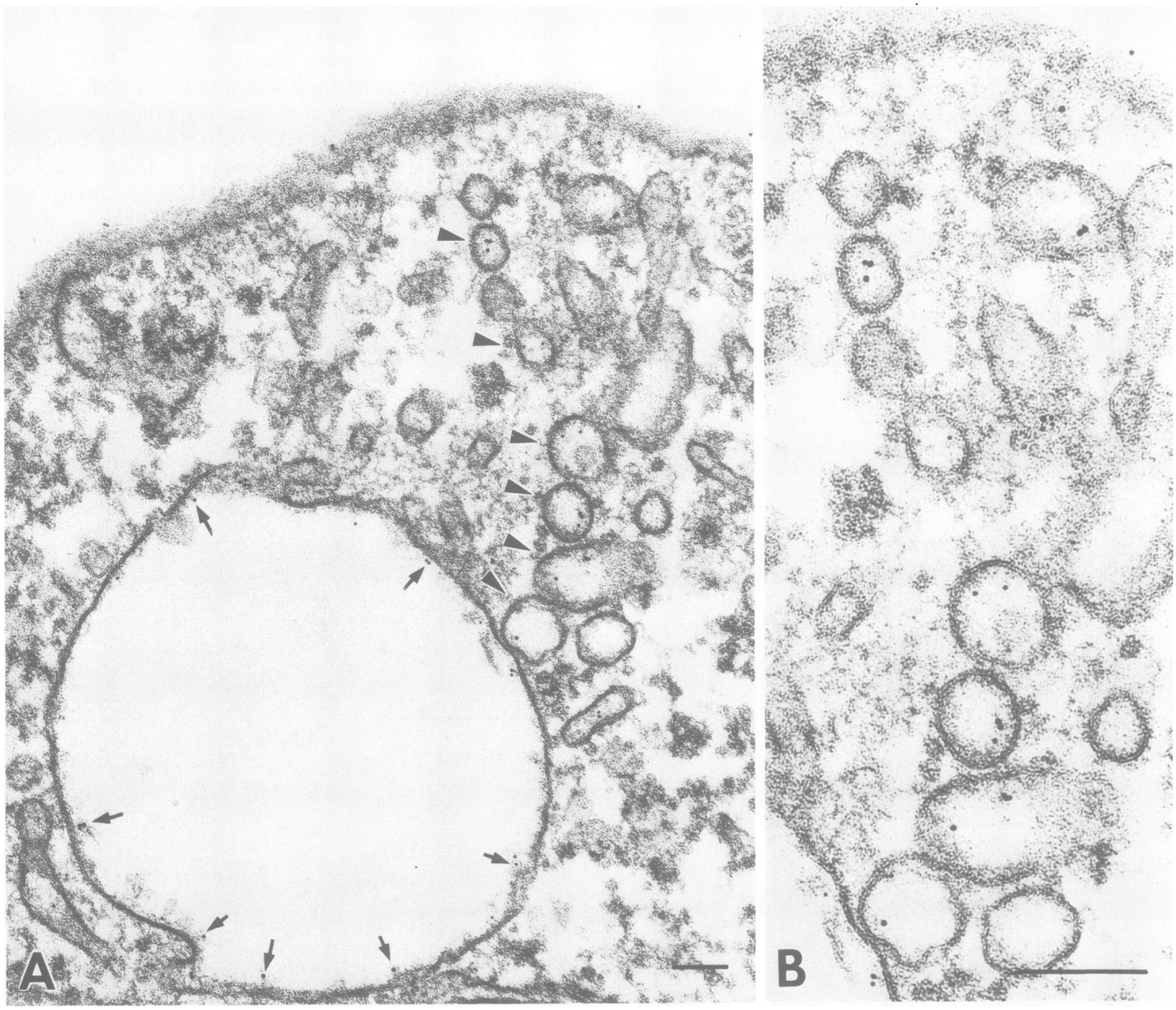

Fig. 10. Localization of CD4DAF by immunoelectron microscopy. The delivery of CD4DAF from the plasma membrane to the prelysosomal compartment (small arrows) seems to be mediated by non-coated vesicles [arrowheads (**A**)]. (**B**) A higher magnification of the non-coated vesicles shown in A. Scale bars = 0.1 μm.

entered the clathrin-coated pit-mediated endocytic pathway and we detected gold particles in endocytic vesicles (1−7 particles per vesicle) (Figure 8B, C and D). Quantitative evaluation indicated that of the labeled vesicles, ~97% were coated and ~3% were non-coated after 5 min at 37°C (Table I). Upon further warming, the proportion of gold labeled CD4 in coated vesicles decreased and we observed labeling of both non-coated vesicles and smooth tubulo-vesicular structures (Figure 8E and F). After 15−18 min at 37°C, 45% of the gold particles were still on the cell surface; the remaining 55% were associated with coated pits, coated vesicles and smooth vesicle profiles. Multivesicular bodies containing label apposed on the membrane of the organelle, or associated with internal material, could be seen after 18−35 min of warming (Figure 8G).

In contrast, the internalization of CD4DAF appeared to be both kinetically and mechanistically different. Endocytosis appeared to be delayed relative to CD4, internalized CD4DAF-associated gold particles being detectable only after ~10 min of warming (Table I). CD4DAF-associated gold particles were seen in non-coated microinvaginations of the plasma membrane (Figure 9B, C and D), while coated vesicles were rarely labeled. This association with non-coated invaginations became pronounced only after warming of the cells to 37°C and particles were still found in non-coated surface invaginations even after 30 min of warming. In addition, small non-coated vesicles (40−100 nm), presumably derived from these invaginations, were localized in the apical and more distal cytoplasm (Figure 10). Large endocytic vesicles and multivesicular bodies were also labeled. Infrequently (~3−4% of labeled vesicles), coated vesicles in the apical cytoplasm contained gold particles. To ensure that coated pits were functional in these cells, the rate of endocytosis of transferrin was measured and found to be indistinguishable in cells expressing CD4DAF versus CD4 (not shown). In addition, immunofluorescent staining with an anti-clathrin monoclonal antibody indicated that the number of clathrin-coated pits and vesicles appeared to be

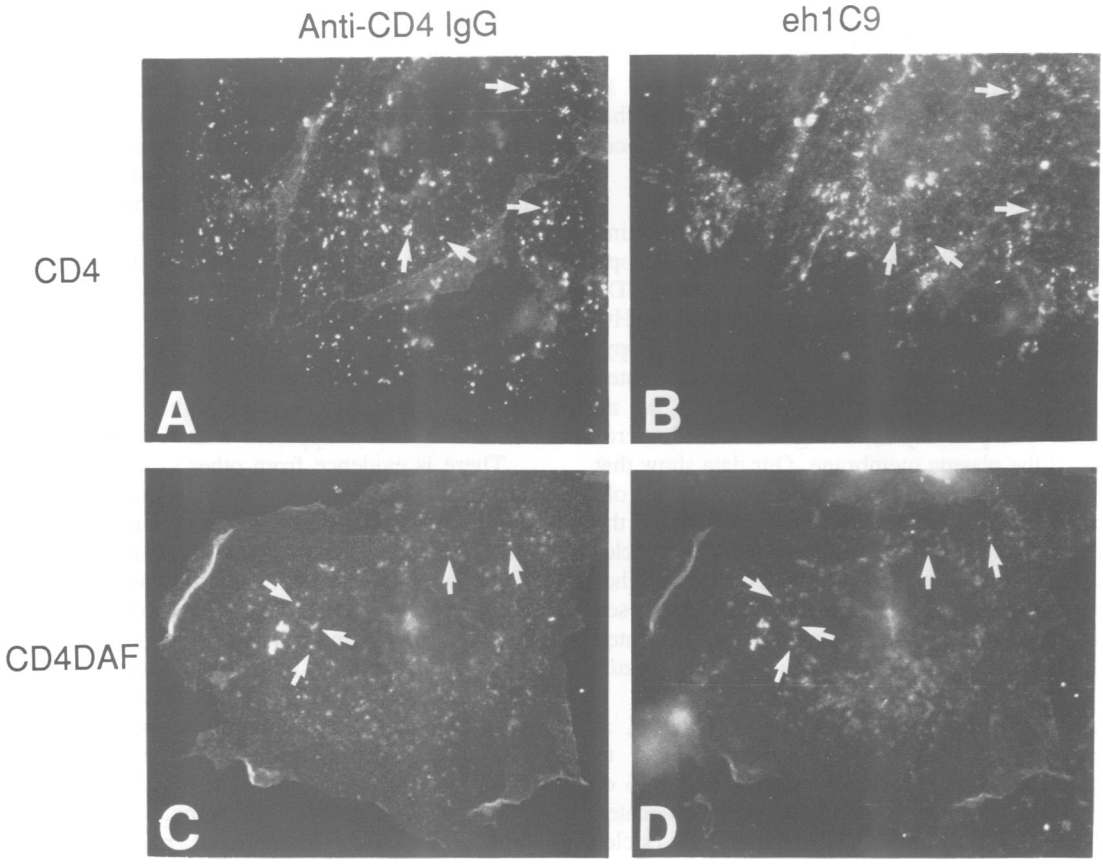

Fig. 11. Internalized CD4 and CD4DAF are delivered to a similar endosomal−lysosomal compartment. Cells expressing either CD4 (**panels A** and **B**) or CD4DAF (panels **C** and **D**) were incubated with rabbit anti-CD4 IgG for 1 h at 4°C and then warmed to 37°C for 40 min. The cells were then fixed, permeabilized and incubated with eh1C9, a monoclonal antibody to a purified CHO cell endosome−lysosome fraction, recognizing gp58, a membrane protein enriched in lysosomes (Schmid, 1990). Internalized anti-CD4 IgG (A and C) and bound eh1C9 (B and D) were visualized following staining with a mixture of fluorescein-conjugated anti-rabbit and rhodamine-conjugated anti-mouse IgGs.

the same in both cell lines (not shown). The above data suggest that whereas CD4 is endocytosed via clathrin-coated pits, CD4DAF appears to be largely excluded from clathrin-coated pits, entering cells by an alternative pathway involving non-coated microinvaginations of the plasma membrane.

It was of interest to ask whether these pathways subsequently converge, both forms of the receptor ultimately being delivered to lysosomes. Cells containing endocytosed anti-CD4 IgG bound to CD4 or CD4DAF were simultaneously stained with a monoclonal antibody, eh1C9, raised against a purified CHO cell endosome−lysosome fraction and recognizing gp58, an integral membrane protein enriched in lysosomes (Schmid, 1990). Internalized IgG bound to either CD4 or CD4DAF co-localized with eh1C9-stained intracellular structures (Figure 11), suggesting that both forms of CD4 are delivered to a similar endosomal−lysosomal compartment.

Discussion

A growing and diverse class of integral membrane proteins is now recognised as being anchored to the plasma membrane by a GPI membrane anchor. The function(s) and consequences of this mode of anchoring, however, remain largely unknown. In this report, we constructed a GPI-linked form of the CD4 receptor and studied its endocytosis in transfected CHO cells, compared to that of transmembrane-anchored CD4.

Kinetics of endocytosis

Our results, using several complementary methods, show that the GPI-linked protein CD4DAF is endocytosed and recycles in transfected CHO cells. Measurements using [^{125}I]gp120 suggest that the rate of endocytosis is ~3-fold slower than that of transmembrane CD4. However, these measurements are complicated by the fact that [^{125}I]gp120 appears to dissociate from the cells upon warming. The total amount of [^{125}I]gp120 internalized into a protease-protected compartment was thus low (10−14% of what was initially surface bound) compared to other examples of receptor-mediated endocytosis (Anderson *et al.*, 1981; Mellman and Plutner, 1984). Dissociation of [^{125}I]gp120 might take place directly from the cell surface before endocytosis occurs or, alternatively, within the low-pH environment of an endosome, followed by recycling and release of gp120 to the medium. The appearance of significant amounts of TCA-precipitable gp120 in the medium supports either of these possibilities. Consistent with the measurements using [^{125}I]gp120, analysis of the cells by both indirect immunofluorescence and electron microscopy indicated that the internalization of CD4DAF is delayed relative to that of CD4. Taken together, these data suggest that the endocytosis

of GPI-linked CD4DAF and transmembrane CD4 proceed with different kinetics, the latter being internalized rapidly and immediately following a temperature shift from 4 to 37°C, whereas the former enters the cell more slowly. In both cases, a plateau is ultimately reached suggesting that the internalized receptors recycle back to the cell surface.

Pathways of endocytosis

The different rates of endocytosis and the different staining patterns observed by immunofluorescence microscopy suggest that GPI-linked CD4DAF and transmembrane CD4 are endocytosed by different pathways in transfected CHO cells. This was corroborated by immunoelectron microscopy, indicating that CD4 is endocytosed via clathrin-coated vesicles while CD4DAF appears to enter cells by an alternative endocytic pathway involving non-coated micro-invaginations of the plasma membrane. Our data show that immediately upon warming (2–5 min at 37°C) gold particles bound to CD4 entered the cells, ~97% of the internalized label being associated with coated pits or vesicles (Figure 8). These results are consistent with data from other systems, suggesting that CD4 is constitutively endoctyosed in transfected, non-lymphoid cells using the clathrin-coated pit-mediated endocytic pathway (Pelchen-Matthews *et al.*, 1991).

In contrast, longer incubation times (~7–10 min, at 37°C) were required before gold particles bound to CD4DAF could be detected inside the cells and ~97% of the internalized particles were associated with non-coated structures. The low density of CD4DAF in coated vesicles (3–4%) suggests that unlike transmembrane CD4, CD4DAF fails to concentrate in coated pits, although CD4DAF molecules may occasionally enter coated pits in a passive process together with bulk membrane components. These observations were not due to a defect in the clathrin pathway since the total number of clathrin-coated pits and vesicles in cells expressing CD4DAF versus CD4 appeared to be similar, as judged by staining of the cells with an anti-clathrin monoclonal antibody, and the measured rate of endocytosis of transferrin appeared to be the same in both cell lines. CD4DAF was found associated with non-coated pinocytotic invaginations in the plasma membrane (Figure 9), suggesting that these are the structures involved in its internalization. Transfer of internalized CD4DAF from the apical cytoplasm to the interior of the cell appeared to be mediated by small non-coated vesicles that possibly fuse together or else deliver their contents to larger vesicles or multivesicular bodies (Figure 10). These observations are consistent with the immunofluorescent staining pattern showing an inward migration of vesicles from the plasma membrane, followed by the appearance of larger vesicles that are perinuclear.

The finding that the GPI-linked protein CD4DAF, which lacks a cytoplasmic tail, fails to be endocytosed through coated pits is compatible with the current view that cytoplasmic domains are important for aggregation in coated pits (Davis *et al.*, 1987; Iacopetta *et al.*, 1988; Lazarovits and Roth, 1988). Consistent with this, two other GPI-linked proteins, Thy-1 (Bretscher *et al.*, 1980) and the folate receptor (Rothberg *et al.*, 1990), have been found to be excluded from clathrin-coated pits, suggesting that this might be a general rule of GPI-linked proteins. Our data indicate that exclusion from clathrin-coated pits slows but does not prevent endocytosis of GPI-linked CD4DAF, which proceeds at a significant rate in CHO cells. In support of this, at least two other GPI-anchored proteins have been shown to undergo endocytosis: 5′-nucleotidase (van den Bosch *et al.*, 1988) and DAF (Tausk *et al.*, 1989). The internalization of both GPI-linked CD4DAF and DAF (Tausk *et al.*, 1989) appears to be different from that of the folate receptor (Rothberg *et al.*, 1990). Whereas the former clearly become internalized in vesicles and larger endosomes within the cytoplasm, the folate receptor remains associated with caveolae at the cell surface, without entering endosomes or lysosomes. Although these caveolae appear morphologically similar to the non-coated invaginations containing CD4DAF, they may be functionally distinct. In addition, the folate receptor appears to be more highly clustered within these structures than is apparent with CD4DAF.

There is evidence from other systems for the existence of a clathrin-independent mechanism of endocytosis. This evidence derives mainly from studies in which receptor-mediated endocytosis was selectively inhibited by potassium depletion, exposure to hypertonic medium, or cytoplasmic acidification, under which conditions cells continued to internalize ricin and fluid-phase markers [reviewed by van Deurs *et al.* (1989)]. In addition, cholera toxin and tetanus toxin, which bind to membrane glycolipids (gangliosides), have been shown by electron microscopy to enter cells via non-coated invaginations of the plasma membrane (Montesano *et al.*, 1982; Tran *et al.*, 1987; Parton *et al.*, 1988). In these studies, gold particles were found associated with non-coated, flask-shaped microinvaginations very similar to the structures containing CD4DAF and, as seen here with CD4DAF, incubation at 37°C resulted in internalization in small non-coated vesicles, followed by later accumulation in multivesicular bodies. In addition, the rate of internalization of cholera toxin was relatively slow (~4-fold slower than that of α2-macroglobulin). The similarity between these results and our observations with CD4DAF is intriguing, suggesting that GPI-linked proteins and ligands bound to membrane glycolipids are internalized by a common pathway, distinct from the coated-pit pathway.

The weak base primaquine has been shown to block the recycling, but not the internalization, of transferrin, asialoglycoprotein and MHC glycoproteins (Schwartz *et al.*, 1984; Stoorvogel *et al.*, 1987; Reid and Watts, 1990). Our data suggest that the recycling of transmembrane CD4 is similarly inhibited by primaquine, leading to higher steady-state levels of internalized ligand. In contrast, the internalization and recycling of CD4DAF appear to be unaffected by primaquine. These data suggest that there may be two populations of early endosomes (the compartment from which recycling is presumed to occur): a primaquine-sensitive population (containing CD4) derived via the clathrin-coated pit-mediated endocytic pathway and a primaquine-insensitive population (containing CD4DAF) derived via endocytosis by an independent mechanism. Of interest in this regard, we note that large tubulo-vesicular structures similar to the organelle proposed to be an intermediate in the recycling of the asialoglycoprotein receptor (Geuze *et al.*, 1983) were highly labeled in cells expressing CD4, but not CD4DAF. Consistent with the above observations, primaquine has been shown to block the recycling of transferrin without inhibiting the recycling of the GPI-anchored protein, 5′-nucleotidase, in rat hepatoma cells (van

den Bosch *et al.*, 1988). It is possible that these observations reflect a relative insensitivity to pH of the clathrin-independent pathway of internalization and recycling. In contrast, clathrin-mediated cycling appears to be pH sensitive, internalization being inhibited by acidification of the cytosol and recycling by weak bases.

Transmembrane CD4 and GPI-linked CD4DAF thus appear to enter cells and recycle using different endocytic pathways. An interesting question is whether these two pathways intersect and, if so, at what point? Co-localization of internalized CD4 and CD4DAF with an antibody raised against a purified endosome−lysosome fraction that recognizes an antigen enriched in lysosomes suggests that the two pathways may converge, both receptors ultimately being transported to the lysosomal compartment. The observation that gold particles bound to either CD4 or CD4DAF appear in multivesicular bodies after prolonged warming is consistent with this view. Similarly, cholera toxin (endocytosed via non-coated vesicles) and α2-macroglobulin (endocytosed through coated vesicles) subsequently associate with the same multivesicular bodies (Tran *et al.*, 1987).

If one excludes the possibility of interactions with other transmembrane proteins, GPI-anchored proteins might be expected to reflect the behavior of the lipid portion of the membrane, endocytosis of the GPI-anchored protein being a consequence of normal turnover of the lipid bilayer. The rate of this turnover could vary depending on the cell type, growth rate, cell cycle, or other factors. As such, GPI-linked proteins could provide useful markers for following the movement and turnover of bulk membrane in the cell.

Materials and methods

Materials

PIPLC purified from *B.thuringiensis* was generously provided by Dr M.G.Low of Columbia University. Monoclonal antibodies against CD4 were provided by K.Rosenthal and B.Fendly of Genentech, Inc. (South San Francisco, CA); the eh1C9 antibody was kindly provided by S.Schmid (Scripps Clinic); purified rgp120 was provided by T.Gregory (Genentech, Inc.); PE-conjugated IgG was from Caltag Laboratories (South San Francisco, CA); IgG coupled to fluorescein or rhodamine and goat anti-transferrin IgG were from Cappel Laboratories (Malvern, PA); gold-conjugated IgG was from Janssen Biotech (Belgium); purified subtilisin was provided by Paul Carter (Genentech, Inc.). Radioiodinated rgp120, prepared as described previously (Smith *et al.*, 1987), was kindly provided by Douglas H.Smith or by Michael Peterson at Genentech, Inc.

Recombinant plasmids and transfections

An expression plasmid encoding the CD4 receptor was provided by Daniel J.Capon at Genentech, Inc. (Smith *et al.*, 1987). To construct CD4DAF, a 2092 bp *Spe*I−*Ava*I fragment (containing the CMV promoter and the coding region for the CD4 extracellular domain) was ligated to a 73 bp *Ava*I−*Xmm*I linker, designed to create an in-frame fusion between the extracellular domain of CD4 and the COOH-terminal 37 residues of DAF. This was gel purified and then ligated to two fragments from a DAF expression plasmid (Caras *et al.*, 1989), a 3790 bp *Spe*I−*Hin*dIII vector fragment and a 453 bp *Hin*dIII−*Xmm*I fragment (containing the 3′-end of DAF). The recombinant plasmid was verified by sequencing. Cells were transfected by the calcium phosphate co-precipitation method (Wigler *et al.*, 1979) using 5−10 μg of plasmid DNA.

Stable expression in CHO cells

Expression plasmids encoding CD4DAF and mouse dihydrofolate reductase (DHFR), a selectable marker for gene expression (Simonsen and Levinson, 1983) were co-transfected into DHFR$^-$ CHO cells. Selected clones were pooled and further selected in medium containing methotrexate (added in stepwise increments from 0.1 to 10 μM). Flow cytometry was used to isolate cells expressing high levels of CD4DAF on their surface and clonal lines were established. A stable cell line expressing CD4 was provided by Scot A.Marsters and Daniel J.Capon at Genentech, Inc. (Lasky *et al.*, 1987).

Internalization assays using [^{125}I]gp120

Cells grown in 100-mm dishes were removed by treatment with 7 mM EDTA in phopshate-buffered saline (PBS) and incubated with ~33 nM (2 μg/ml) [^{125}I]gp120 (~8700 c.p.m./ng) for 2 h at 4°C in Dulbecco's modified Eagle medium (DMEM) containing 4% fetal calf serum (FCS). After washing with cold medium to remove unbound ligand, the cells were warmed to 37°C for various times and then chilled. To distinguish between surface-bound and intracellular radiolabel, the cells were treated with subtilisin (0.5 mg/ml) in buffer containing 140 ml NaCl, 2 mM KCl, 10 mM $MgCl_2$, 20 mM Tris−HCl (pH 7.5), 10% sucrose and 1 mM DTT for 2 h at 4°C. This treatment removed 96−97% of the radiolabel from cells held at 4°C, where all of the bound radiolabel is presumably on the cell surface. Non-specific binding was assessed by determining the amount of radiolabel bound in the presence of 600 μg/ml of unlabeled rgp120. To measure ligand degradation, the cells and media were separated by centrifugation. The media (800 μl) were centrifuged a second time, added to 150 μl of ice-cold 100% TCA and incubated on ice for 1 h. The TCA-precipitated proteins were removed by centrifugation and the amount of radiolabel in the supernatants was determined.

Flow cytometry

Cells were incubated with anti-CD4 IgG (~2 μg/10^6 cells) for 1 h at 4°C and then washed with cold DMEM/2% FCS. The cells were then either held on ice or incubated at 37°C or treated with PIPLC. Anti-CD4 IgG complexes on the cell surface were detected by incubating the cells with PE-conjugated goat anti-mouse IgG for 30 min at 4°C. The fluorescence intensity was measured on a Coulter Elite flow cytometer.

Immunofluorescence microscopy

Cells grown on coverslips were incubated with anti-CD4 IgG for 1 h on ice and then warmed to 37°C for various times. Cells were then fixed with cold 3.7% formaldehyde in PBS, permeabilized with 0.5% Triton X-100 in PBS, and incubated with rhodamine- or fluorescein-conjugated anti-mouse IgG for 30 min at room temperature. In some instances, cells were additionally incubated with a monoclonal antibody against a lysosomal fraction (Schmid, 1990) following permeabilization. The cells were washed with PBS and mounted in 90% glycerol/100 mM Tris (pH 8.5) containing 0.1% *p*-phenylenediamine as an anti-bleaching agent. Immunofluoresence was performed on a Zeiss photoscope III microscope.

Immunogold labeling and electron microscopy

Cells grown in 35-mm dishes were incubated with anti-CD4 IgG followed by 5 nm gold-conjugated anti-mouse IgG at 4°C for 2 h. The cells were then warmed to 37°C for 0−35 min and fixed in 1% formaldehyde, 1.5% glutaraldehyde in 0.1 M cacodylate buffer (pH 7.2) for 2 h. They were then post-fixed in 2% osmium in the same buffer, stained en bloc overnight in aqueous uranyl acetate and dehydrated in a graded ethanol series. The cells were then removed from the dishes with propylene oxide and embedded in Epon 812. Ultrathin sections were obtained in a Reichert Ultracut E microtome and counterstained with aqueous uranyl acetate and lead citrate. The grids were observed in a Philips CM 12 electron microscope.

PIPLC digestions

Cells were treated with purified PIPLC from *B.thuringiensis*, ~4 μg/ml in DMEM/2% FCS, for 2 h at 4°C.

Metabolic labeling and immunoprecipitations

Labeling with [^{35}S]methionine and immunoprecipitation were as previously described (Caras *et al.*, 1989).

Acknowledgements

We thank Frances Brodsky, Kim Rosenthal, Brian Fendly, Douglas Smith, Michael Peterson, Tim Gregory, Daniel Capon and Paul Carter for supplying valuable reagents.

References

Anderson,R.G.W., Brown,M.S. and Goldstein,J.L. (1981) *J. Cell Biol.*, **88**, 441−452.

Bangs,J.D., Hereld,D., Krakow,J.L., Hart,G.W. and Englund,P.T. (1985) *Proc. Natl. Acad. Sci. USA*, **82**, 3207−3211.

Bangs,J.D., Andrews,N.W., Hart,G.W. and Englund,P.T. (1986) *J. Cell Biol.*, **103**, 255–263.
Bretscher,M.S.. Thomson,J.N. and Pearse,B.M.F. (1980) *Proc. Natl. Acad. Sci. USA*, **77**, 4156–4159.
Caras,I.W., Weddell,G.N., Davitz,M.A., Nussenzweig,V. and Martin,D.W.,Jr (1987) *Science*, **238**, 1280–1283.
Caras,I.W., Weddell,G.N. and Williams.S.R. (1989) *J. Cell Biol.*, **108**, 1387–1396.
Cross,G.A.M. (1990) *Annu. Rev. Cell Biol.*, **6**, 1–39.
Davis,C.G., van Driel,I.R., Russel,D.W., Brown,M.S. and Goldstein,J.L. (1987) *J. Biol. Chem.*, **262**, 4075–4082.
Ferguson,M.A.J. and Williams,A.F. (1988) *Annu. Rev. Biochem.*, **57**, 285–320.
Ferguson,M.A.J., Duszenko,M., Lamont,G.S., Overath,P. and Cross,G.A.M. (1986) *J. Biol Chem.*, **261**, 356–362.
Geuze,H.J., Slot,J.W. and Strous,G.J.A.M. (1983) *Cell*, **32**, 277–287.
Iacopetta,B.J., Rothenberger,S. and Kühn,L.C. (1988) *Cell*, **54**, 485–489.
Klatzman,D., Champagne,E., Chamaret,S., Gruest,J., Guetard,D., Hercend,T., Gluckman,J.-C. and Montagnier,L. (1984) *Nature*, **312**, 767–768.
Lasky,L.A., Nakamura,G., Smith,D.H., Fennie,C., Shimasaki,C., Patzer,E., Berman,P., Gregory,T.G. and Capon,D.J. (1987) *Cell*, **50**, 975–985.
Lazarovits,J. and Roth,M. (1988) *Cell*, **53**, 743–752.
Lemansky,P., Fatemi,S.H., Gorican,B., Meyale,S., Rossero,R. and Tartakoff,A.M. (1990) *J. Cell Biol.*, **110**, 1525–1531.
Low,M.G. (1989) *FASEB J.*, **3**, 1600–1608.
Low,M.G. and Kincade,P.W. (1985) *Nature*, **318**, 62–64.
Maddon,P.J., Littman,D.R., Godfrey,M., Maddon,D.E., Chess,L. and Axel,R. (1985) *Cell*, **42**, 93–104.
McDougal,J.S., Kennedy,M.S., Sligh,J.M., Cort,S.P., Mawle,A. and Nicholson,J.K.A. (1986) *Science*, **231**, 382–385.
Mellman,I. and Plutner,H. (1984) *J. Cell Biol.*, **98**, 1170–1177.
Montesano,R., Roth,J., Robert,A. and Orci,L. (1982) *Nature*, **296**, 651–653.
Munson,P.J. and Rodbard,D. (1980) *Anal. Biochem.*, **107**, 220–239.
Parton,R.G., Ockleford,C.D. and Critchley,D.R. (1988) *Brain Res.*, **475**, 118–127.
Pelchen-Matthews,A., Armes,J.E. and Marsh,M. (1989) *EMBO J.*, **8**, 3641–3649.
Pelchen-Matthews,A., Armes,J.E., Griffiths,G. and Marsh,M. (1991) *J. Exp. Med.*, **173**, 575–587.
Reid,P.A. and Watts,C. (1990) *Nature*, **346**, 655–657.
Rothberg,K.G., Ying,Y., Kolhouse,J.F., Kamen,B.A. and Anderson,R.G.W. (1990) *J. Cell Biol.*, **110**, 637–649.
Schmid,S. (1990) In Hilderson,H.J. (ed.), *Subcellular Biochemistry*. Vol. 16.
Schwartz,A.L., Bolognesi,A. and Fridovich,S.E. (1984) *J. Cell Biol.*, **98**, 732–738.
Simonsen,C.C. and Levinson,A.D. (1983) *Proc. Natl. Acad. Sci. USA*, **80**, 2495–2499.
Smith,D.H., Byrn,R.A., Marsters,S.A., Gregory,T., Groopman,J.E. and Capon,D.J. (1987) *Science*, **238**, 1704–1707.
Stoorvogel,W., Geuze,H.J. and Strous,G.J. (1987) *J. Cell Biol.*, **104**, 1261–1268.
Tausk,F., Fey,M. and Gigli,I. (1989) *J. Immunol.*, **143**, 3295–3302.
Tran,D., Carpentier,J.-L., Sawano,F., Gorden,P. and Orci,L. (1987) *Proc. Natl. Acad. Sci. USA*, **84**, 7957–7961.
van den Bosch,R., du Maine,A.P.M., Geuze,H.J., van der Ende,A. and Strous,G.J. (1988) *EMBO J.*, **7**, 3345–3351.
van Deurs,B., Petersen,O.W., Olsnes,S. and Sandvig,K. (1989) *Int. Rev. Cytol.*, **117**, 131–177.
Wigler,M., Pellicer,A., Silverstein,S., Axel,R., Urlaub,G. and Chasin,L. (1979) *Proc. Natl. Acad. Sci. USA*, **76**, 1373–1376.

Received on August 7, 1991; revised on November 18, 1991